Zeitschrift: Bulletin der Schweizerischen Akademie der Medizinischen Wissenschaften = Bulletin de l'Académie suisse des sciences médicales = Bollettino dell' Accademia svizzera delle scienze mediche

Herausgeber: Schweizerische Akademie der Medizinischen Wissenschaften

Band: 36 (1980)

Artikel: Local cerebral energy metabolism : its relationships to local functional activity and blood flow

Autor: Sokoloff, Louis

DOI: https://doi.org/10.5169/seals-308228

Bull. Schweiz. Akad. Med. Wiss. 36, 71-91 (1980)

Laboratory of Cerebral Metabolism, National Institute of Mental Health, United States Public Health Service, Department of Health, Education, and Welfare, Bethesda, Maryland

LOCAL CEREBRAL ENERGY METABOLISM: ITS RELATIONSHIPS TO LOCAL FUNCTIONAL ACTIVITY AND BLOOD FLOW

LOUIS SOKOLOFF

Abstract

The results of studies with the (^{14}C)deoxyglucose technique unequivocally establish that local energy metabolism in cerebral tissues is, as in other tissues, closely coupled to local functional activity. Stimulation of local functional activity increases the local rate of glucose utilization; reduced functional activity depresses it. Local cerebral blood flow is normally distributed among the cerebral structures in almost exact proportion to their rates of glucose utilization and changes together with local glucose consumption in response to altered local functional activity. These results demonstrate that the level of functional activity in the structural and functional components of the central nervous system regulates the local rate of energy metabolism, and local blood flow is adjusted to the local metabolic demand.

Zusammenfassung

Der lokale Energiestoffwechsel des Hirngewebes ist – wie Untersuchungen mit der C^{14} Desoxyglucosemethode eindeutig zeigen – eng mit der lokalen Hirnaktivität gekoppelt. Eine Steigerung der Hirnaktivität erhöht den Glucoseverbrauch, eine Abnahme geht mit einer Verminderung derselben einher. Die regionale cerebrale Durchblutung ist im Normalfall proportional zum lokalen Glucoseverbrauch und ändert sich entsprechend dem Aktivitätsniveau. Die Untersuchungen zeigen, dass die lokale Hirnaktivität (strukturell und funktionell) den regionalen Energiestoffwechsel reguliert, wobei sich der lokale Blutfluss nach dem lokalen Energiebedarf richtet.

The concept that the regulation of the cerebral circulation is at least in part mediated by the products of cerebral metabolism and that cerebral blood flow is adjusted to local cerebral metabolism and functional activity is almost a century old. In a classic paper published in 1890, ROY and SHERRINGTON (1890) stated, "... the chemical products of cerebral metabolism contained in the lymph which bathes the walls of the arterioles of the brain can cause variations of the calibre of the cerebral vessels ... in this re-action the brain possesses an intrinsic mechanism by which its vascular supply can be varied locally in correspondence with local variations of functional activity." The validity of this hypothesis has been generally assumed, and it has been the basis of many of our current ideas about the regulation of the cerebral circulation. Direct experimental evidence in support of it, however, has awaited the development of methods for the measurement of blood flow and energy metabolism in discrete structural components of the brain exhibiting alterations in functional activity.

Methods for the determination of local cerebral blood flow in conscious laboratory animals have been available for at least 20 years. The autoradiographic inert gas technique was originally designed for use with the radioactive inert gas, (^{131}I)trifluoroiodomethane (LANDAU et al., 1955); this method provided the means to measure the rates of blood flow simultaneously in all the macroscopic structures of the brain visible on autoradiographs (LANDAU et al. 1955; FREYGANG and SOKOLOFF 1958). In order to avoid the technical difficulties associated with the use of a volatile tracer, the method was modified for use with the non-volatile tracer, (^{14}C)antipyrine (REIVICH et al. 1969). The diffusion of (^{14}C)-antipyrine across the blood-brain barrier has been found, however, to be too restricted to permit purely blood flow-limited uptake by the cerebral tissues, and its use leads to underestimates of local cerebral blood flow (ECKMAN et al. 1975). This limitation has recently been overcome by the use of (^{14}C)iodoantipyrine, an analogue with far more rapid diffusion through the blood-brain barrier, which provides values for local cerebral blood flow essentially the same as those obtained originally with the (^{131}I)trifluoroiodomethane (SAKURADA et al. 1978).

These autoradiographic methods have been used to demonstrate that local blood flow in the brain is indeed altered in response to changes in local functional activity. For example, retinal stimulation by light has been found to increase blood flow in discrete regions of the central visual pathways of the cat, for example, the lateral geniculate ganglion, superior colliculus, and visual cortex (SOKOLOFF 1961). Because the cerebral circulatory response was slow, it was presumed that the mechanism of the regulation was chemical, possibly mediated by the products of metabolism. There was, however, no demonstration that local energy metabolism is coupled to local functional activity in the brain as it is in other tissues.

The recently developed (^{14}C)deoxyglucose method (SOKOLOFF et al. 1977) has provided the last link needed to study the relationships among local functional activity, energy metabolism, and blood flow in the brain. This method can be used to measure quantitatively the local rates of glucose utilization simultaneously in all the macroscopically visible structures of the brain. It can be applied to normal conscious animals as well as those in experimentally altered states of cerebral activity. Furthermore, the (^{14}C)deoxyglucose method also employs an autoradiographic technique which provides pictorial representations of the relative rates of glucose utilization throughout the various components of the brain; even without quantification these autoradiographs provide clearly visible markers that map cerebral regions with increased or decreased rates of energy metabolism in altered physiological, pharmacological, and pathological states. This method has provided unequivocal evidence of a close relationship between functional activity and energy metabolism in discrete structural and/or functional units of the nervous system (SOKOLOFF, 1977), and together with the local blood flow techniques has demonstrated the remarkably close correlation between local blood flow and energy metabolism.

Methods

The application of quantitative autoradiographic techniques for the measurement of local tissue concentrations of chemically inert, radioactive, diffusible tracers has made it possible to determine the rates of blood flow simultaneously in most of the individual structural and functional components of the brain (LANDAU et al. 1955; REIVICH et al. 1969; SAKURADA, 1978). The extension of quantitative autoradiography to the determination of local cerebral metabolic rate with the same degree of anatomical resolution has proved to be more difficult because of the inherently greater theoretical complexity of the problem and the unsuitability of the radioactive species of the usual substrates of cerebral energy metabolism, oxygen and glucose. The radioisotopes of oxygen have too short a physical half-life, and the labeled products of the metabolism of both oxygen and glucose have too short a biological half-life in the cerebral tissues. We have, therefore, employed 2-(^{14}C)deoxyglucose, an analogue of glucose with special properties that make it particularly appropriate to trace glucose metabolism and to measure the rates of local glucose consumption within the various functional and structural components of the brain. Like the local cerebral blood flow techniques, the method is applicable to conscious as well as anesthetized laboratory animals.

Theory

2-Deoxy-D-glucose (DG) is transported from blood to brain by the same carrier that transports glucose, and like glucose it is phosphorylated in the cerebral tissues by hexokinase. Deoxyglucose and glucose are, therefore, competitive substrates for both transport and hexokinase-catalyzed phosphorylation. Unlike glucose-6-phosphate (G-6-P), however, which is rapidly metabolized further to CO_2 and H_2O, 2-deoxyglucose-6-phosphate (DG-6-P) cannot be converted to fructose-6-phosphate by phosphohexoseisomerase and is, therefore, essentially trapped in the tissues, at least for the intervals of time that concern us. We have determined the half-lives of (^{14}C)DG-6-P in various cerebral tissues and found none shorter than six hours (SOKOLOFF et al. 1977). When (^{14}C)DG is introduced into the circulation, the amount of (^{14}C)DG-6-P accumulated in any cerebral tissue et any time later equals the integral of the rate of (^{14}C)DG phosphorylation with respect to time in that tissue, and this quantity is in turn quantitatively related to the amount of glucose that has been phosphorylated over the same time period, depending on the time course of the relative concentrations of (^{14}C)DG and glucose in the precursor pools and the kinetic constants for hexokinase with respect to both DG and glucose. With cerebral glucose utilization in a steady state, the amount of glucose phosphorylated during the interval of time equals the steady state flux of glucose through the hexokinase-catalyzed step times the duration of the interval, and the net flux of glucose through this step equals the rate of glucose utilization.

It is beyond the scope of this report to present the details of the model and the theoretical analyses which form the basis of this method. These are presented elsewhere (SOKOLOFF et al. 1977). Briefly, the basic principles are as follows. The model assumes a steady state for glucose (i.e., constant plasma glucose concentration and constant rates of tissue glucose consumption) throughout the period of the procedure, homogeneous tissue compartments within which the precursor concentrations of (^{14}C)DG and glucose are uniform and exchange directly with the plasma, and tracer concentrations of (^{14}C)DG (i.e., molecular concentrations of free (^{14}C)DG essentially equal to zero). Mathematical analysis of the model leads to the following equation:

$$R_i = \frac{C_i^*(T) - k_1^* e^{-(k_2^* + k_3^*)T} \int_0^T C_P^* e^{(k_2^* + k_3^*)t} dt}{\left[\frac{\lambda V_m^* K_m}{\Phi V_m K_m^*}\right] \left[\int_0^T (C_P^*/C_P)dt - e^{-(k_2^* + k_3^*)T} \int_0^T (C_P^*/C_P) e^{(k_2^* + k_3^*)t} dt\right]}$$

where R_i equals the calculated rate of glucose utilization per gram of tissue, i; T equals time of killing; $C_i^*(T)$ equals the total concentration of (^{14}C)DG and (^{14}C)DG-6-P in tissue, i, at time, T, determined by quantitative autoradiography; C_p^* and C_p equal the arterial plasma concentrations of (^{14}C)DG and glucose, respectively; k_1^*, k_2^*, and k_3^* are the rate constants for the transport of (^{14}C)DG from the plasma to the tissue precursor pool, for its transport back from tissue to plasma, and for the phosphorylation of free (^{14}C)DG in the tissue, respectively; λ equals the ratio of the distribution space of (^{14}C)DG in the tissue to that of glucose; Φ equals the fraction of glucose which once phosphorylated continues down the glycolytic pathway; and K_m^* and V_{max}^* and K_m and V_{max} are the familiar Michaelis-Menten kinetic constants of hexokinase for (^{14}C)DG and glucose, respectively.

The rate constants are determined in a separate group of animals by a non-linear, iterative, computer-routine which provides the best-fit of the experimentally determined time courses of tissue and plasma ^{14}C concentrations to an equation which defines the time course of tissue concentration in terms of the time, the history of the plasma concentration, and the rate constants (SOKOLOFF et al. 1977). The λ, Φ, and the enzyme kinetic constants are grouped together to constitute a single, lumped constant (see equation). It can be shown mathematically that this lumped constant is equal to the asymptotic value of the product of the ratio of the cerebral extraction ratios of (^{14}C)DG and glucose and the ratio of the arterial blood to plasma specific activities when the arterial plasma (^{14}C)DG concentration is maintained constant. The lumped constant is also determined in a separate group of animals from arterial and cerebral venous blood samples drawn during a programmed intravenous infusion which produces and maintains a constant arterial plasma (^{14}C)DG concentration (SOKOLOFF et al. 1977). These essential constants have thus far been determined in the rat, Rhesus monkey, cat, and Beagle puppy (SOKOLOFF, 1979).

Procedure

The procedure is to inject a pulse of (^{14}C)DG intravenously at zero time and to decapitate the animal at a measured time, T, 30–45 minutes later; in the interval timed arterial samples are taken for the measurement of the time courses of the plasma (^{14}C)DG and glucose concentrations. Tissue ^{14}C concentrations are measured at time, T, by the quantitative autoradiographic technique (REIVICH et al. 1969; SOKOLOFF et al. 1977). The local rates of glucose utilization are calculated from these measured variables by means of the operational equation.

Table 1. Representative values for local cerebral glucose utilization in the normal conscious albino rat and monkey (μmol/100 g/min).

Structure	Albino rat* (n = 10)	Monkey ** (n = 7)
Gray Matter		
Visual cortex	107 ± 6	59 ± 2
Auditory cortex	162 ± 5	79 ± 4
Parietal cortex	112 ± 5	47 ± 4
Sensory-motor cortex	120 ± 5	44 ± 3
Thalamus: lateral nucleus	116 ± 5	54 ± 2
Thalamus: ventral nucleus	109 ± 5	43 ± 2
Medial geniculate body	131 ± 5	65 ± 3
Lateral geniculate body	96 ± 5	39 ± 1
Hypothalamus	54 ± 2	25 ± 1
Mamillary body	121 ± 5	57 ± 3
Hippocampus	79 ± 3	39 ± 2
Amygdala	52 ± 2	25 ± 2
Caudate-putamen	110 ± 4	52 ± 3
Nucleus accumbens	82 ± 3	36 ± 2
Globus pallidus	58 ± 2	26 ± 2
Substantia nigra	58 ± 3	29 ± 2
Vestibular nucleus	128 ± 5	66 ± 3
Cochlear nucleus	113 ± 7	51 ± 3
Superior olivary nucleus	133 ± 7	63 ± 4
Inferior colliculus	197 ± 10	103 ± 6
Superior colliculus	95 ± 5	55 ± 4
Pontine gray matter	62 ± 3	28 ± 1
Cerebellar cortex	57 ± 2	31 ± 2
Cerebellar nuclei	100 ± 4	45 ± 2
White matter		
Corpus callosum	40 ± 2	11 ± 1
Internal capsule	33 ± 2	13 ± 1
Cerebellar white matter	37 ± 2	12 ± 1

The values are the means ± standard errors from measurements made in the number of animals indicated (n).
* From SOKOLOFF et al. (1977).
** From KENNEDY et al. (1978).

Normal rates of local cerebral glucose utilization in the rat and monkey

The most extensive determinations of the local rates of cerebral glucose utilization have been made in the albino rat and Rhesus monkey. The rates in the normal conscious rat vary widely throughout the brain with the values in white matter distributed in a narrow low range and the values in gray structures broadly distributed around an average which is about three times greater than that of white matter (Table 1). The highest values are in structures of the auditory system, with the inferior colliculus clearly the most metabolically active structure in the brain (Table 1).

Table 2. Effects of thiopental anesthesia on local cerebral glucose utilization in the albino rat*+.

Structure	Local cerebral glucose utilization (μmoles/100 g/min) Control (6)**	Anesthetized (8)**	% Effect
Gray Matter			
Visual cortex	111 ± 5	64 ± 3	- 42
Auditory cortex	157 ± 5	81 ± 3	- 48
Parietal cortex	107 ± 3	65 ± 2	- 39
Sensory-motor cortex	118 ± 3	67 ± 2	- 43
Lateral geniculate body	92 ± 2	53 ± 3	- 42
Medial geniculate body	126 ± 6	63 ± 3	- 50
Thalamus: lateral nucleus	108 ± 3	58 ± 2	- 46
Thalamus: ventral nucleus	98 ± 3	55 ± 1	- 44
Hypothalamus	63 ± 3	43 ± 2	- 32
Caudate-putamen	111 ± 4	72 ± 3	- 35
Hippocampus : ammon's horn	79 ± 1	56 ± 1	- 29
Amygdala	56 ± 4	41 ± 2	- 27
Cochlear nucleus	124 ± 7	79 ± 5	- 36
Lateral lemniscus	114 ± 7	75 ± 4	- 34
Inferior colliculus	198 ± 7	131 ± 8	- 34
Superior olivary nucleus	141 ± 5	104 ± 7	- 26
Superior colliculus	99 ± 3	59 ± 3	- 40
Vestibular nucleus	133 ± 4	81 ± 4	- 39
Pontine gray matter	69 ± 3	46 ± 3	- 33
Cerebellar cortex	66 ± 2	44 ± 2	- 33
Cerebellar nucleus	106 ± 4	75 ± 4	- 29
White Matter			
Corpus callosum	42 ± 2	30 ± 2	- 29
Genu of corpus callosum	35 ± 5	30 ± 2	- 14
Internal capsule	35 ± 2	29 ± 2	- 17
Cerebellar white matter	38 ± 2	29 ± 2	- 24

* Determined at 30 minutes following pulse of (^{14}C)deoxyglucose.

** The values are the means ± standard errors obtained in the number of animals indicated in parentheses. All the differences are statistically significant at the $p < 0.05$ level.

+From SOKOLOFF et al. (1977).

The rates of local cerebral utilization in the conscious monkey exhibit similar heterogeneity, but they are generally one-third to one-half of the values in corresponding structures of the rat brain (Table 1). The differences in rates in the rat and monkey brain are consistent with the different cellular packing densities in the brains of these two species.

There are no available data for comparison, but the values in the rat appear to be close to those to be expected from the average metabolic rates determined by EKLÖF et al. (1973) in the rat cerebral cortex and by NILSSON and SIESJÖ (1976) in the rat brain as a whole.

Similarly, the values of the monkey agree closely with those to be expected from the average values obtained by SCHMIDT, KETY and PENNES (1945) in the brain as a whole of the lightly anesthetized monkey.

Effects of anesthesia

General anesthesia induced by thiopental reduces the rates of glucose utilization in all structures of the rat brain (Table 2). The effects are not uniform, however. The greatest reductions occur in the gray structures, particularly those of the primary sensory pathways. The effects in white matter, though definitely present, are relatively small compared with those in gray matter.

Relationship between local functional activity and energy metabolism

The results of a variety of applications of the method demonstrate a clear relationship between local cerebral functional activity and glucose utilization. The most striking demonstrations of the close coupling between function and energy metabolism are seen with experimentally induced local alterations in functional activity that are restricted to a few specific areas in the brain. The effects on local glucose consumption are then so pronounced that they are not only observed in the quantitative results but can be visualized directly in the autoradiographs, which are really pictoral representations of the relative rates of glucose utilization in the various structural components of the brain.

Effects of Increased Functional Activity

Effects of Electrical Stimulation. Fig. 1 illustrates the effects of increased neural activity resulting from electrical stimulation of the sciatic nerve in the rat under barbiturate anesthesia. Such stimulation of one sciatic nerve causes pronounced increases in glucose consumption (i.e., increased optical density in the autoradiographs) in the ipsilateral dorsal horn of the lumbar spinal cord (KENNEDY et al. 1975). No such asymmetry occurs in the spinal cord of unstimulated control animals.

Effects of Experimental Focal Seizures. The local injection of 25,000 units of potassium benzyl penicillin into the hand-face area of the motor cortex of the Rhesus monkey has been shown to induce electrical discharges in the adjacent cortex and to result in recurrent focal seizures involving the face, arm, and hand on the contralateral side (CAVENESS, 1969). Such seizure activity causes selective increases in glucose consumption in areas of motor cortex adjacent to the penicillin locus and in small discrete regions of the putamen, globus pallidus, caudate nucleus, thalamus, and substantia nigra of the same side (Fig. 2) (KENNE-

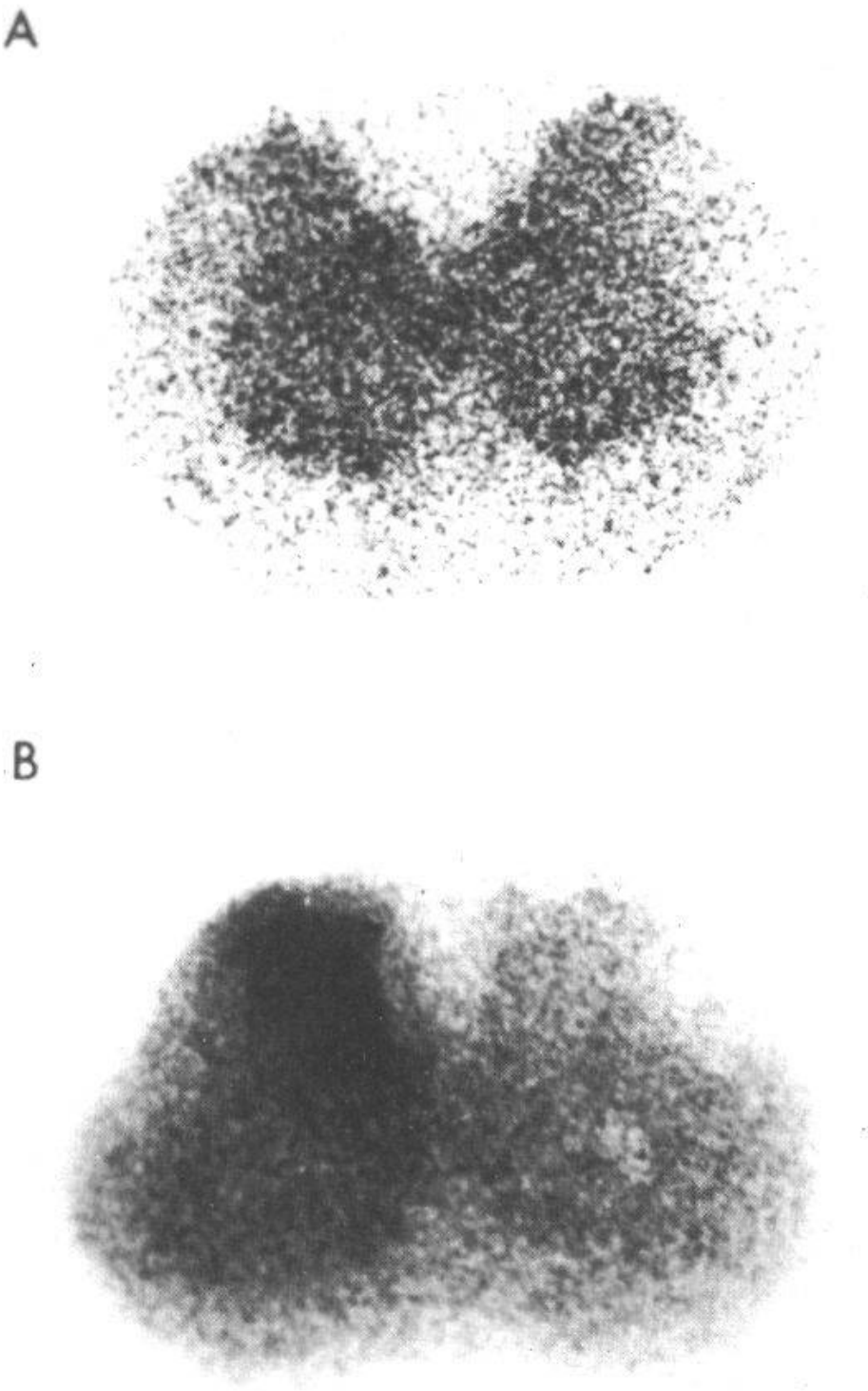

Fig. 1. Effects of increased functional activity in lumbar spinal cord produced by unilateral electrical stimulation of sciatic nerve on local tissue glucose utilization. (A) Autoradiograph of section of lumbar spinal cord from control rat. (B) Autoradiograph of section of lumbar spinal cord from rat with unilateral electrical stimulation of sciatic nerve. Note bilateral symmetry of optical densities in control rat (A) and asymmetrical increase in optical density in dorsal horn ipsilateral to side of stimulation in animal with sciatic nerve stimulation (B). From KENNEDY et al. (1975).

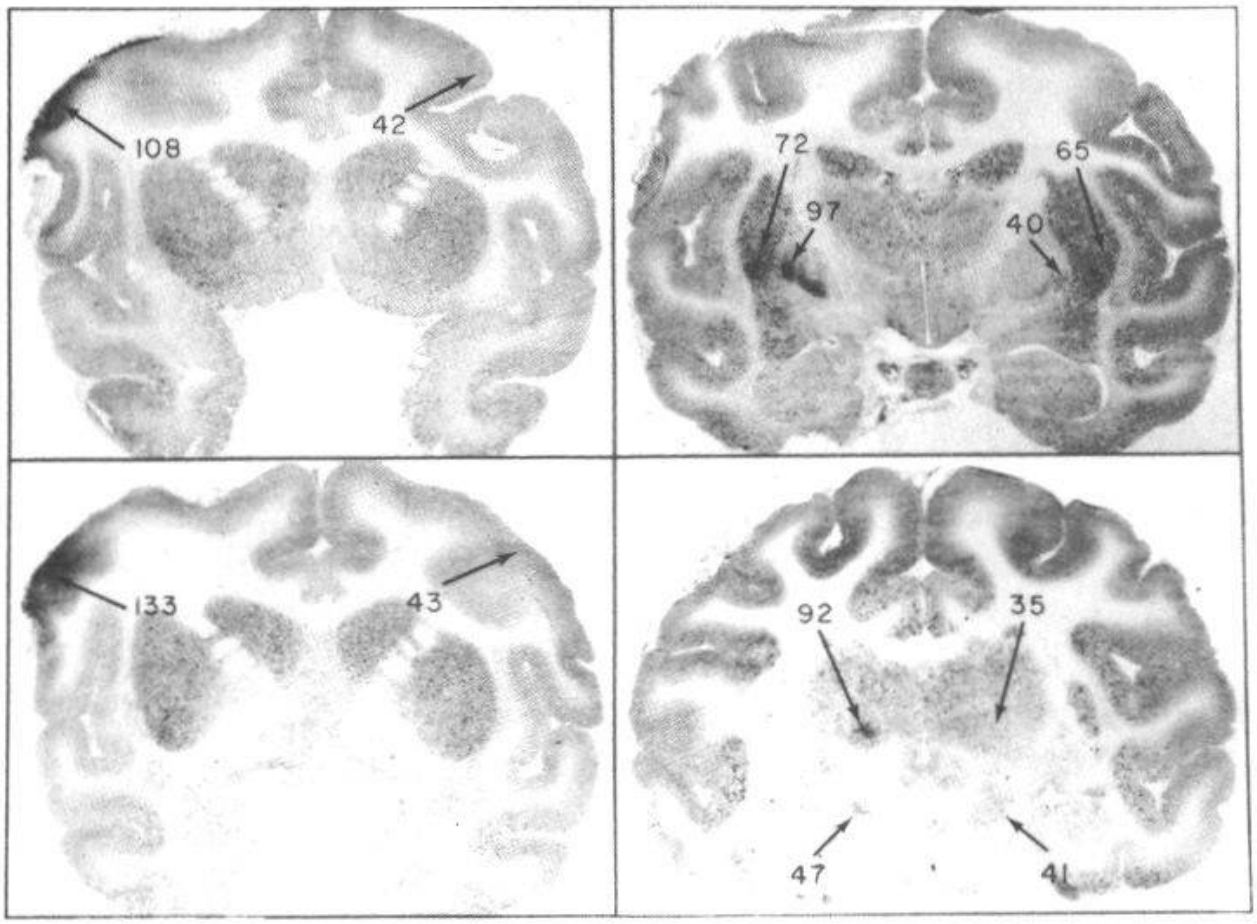

LOCAL GLUCOSE UTILIZATION DURING FOCAL SEIZURE (μmoles/100g/min)

Fig. 2. Effects of focal seizures produced by local application of penicillin to motor cortex on local cerebral glucose utilization in the Rhesus monkey. The penicillin was applied to the hand and face area of the left motor cortex. The left side of the brain is on the left in each of the autoradiographs in the figure. The numbers are the rates of local cerebral glucose utilization in μmoles/100 g tissue/min., calculated according to the operational equation presented in the text. Note the following: Upper left, motor cortex in region of penicillin application and corresponding region of contralateral motor cortex; lower left, ipsilateral and contralateral motor cortical regions remote from area of penicillin applications; upper right, ipsilateral and contralateral putamen and globus pallidus; lower right, ipsilateral and contralateral thalamic nuclei and substantia nigra. From KENNEDY et al. (1975).

DY et al. 1975). Similar studies in the rat have led to comparable results and provided evidence on the basis of an evoked metabolic response of a "mirror" focus in the motor cortex contralateral to the penicillin-induced epileptogenic focus (COLLINS et al. 1976).

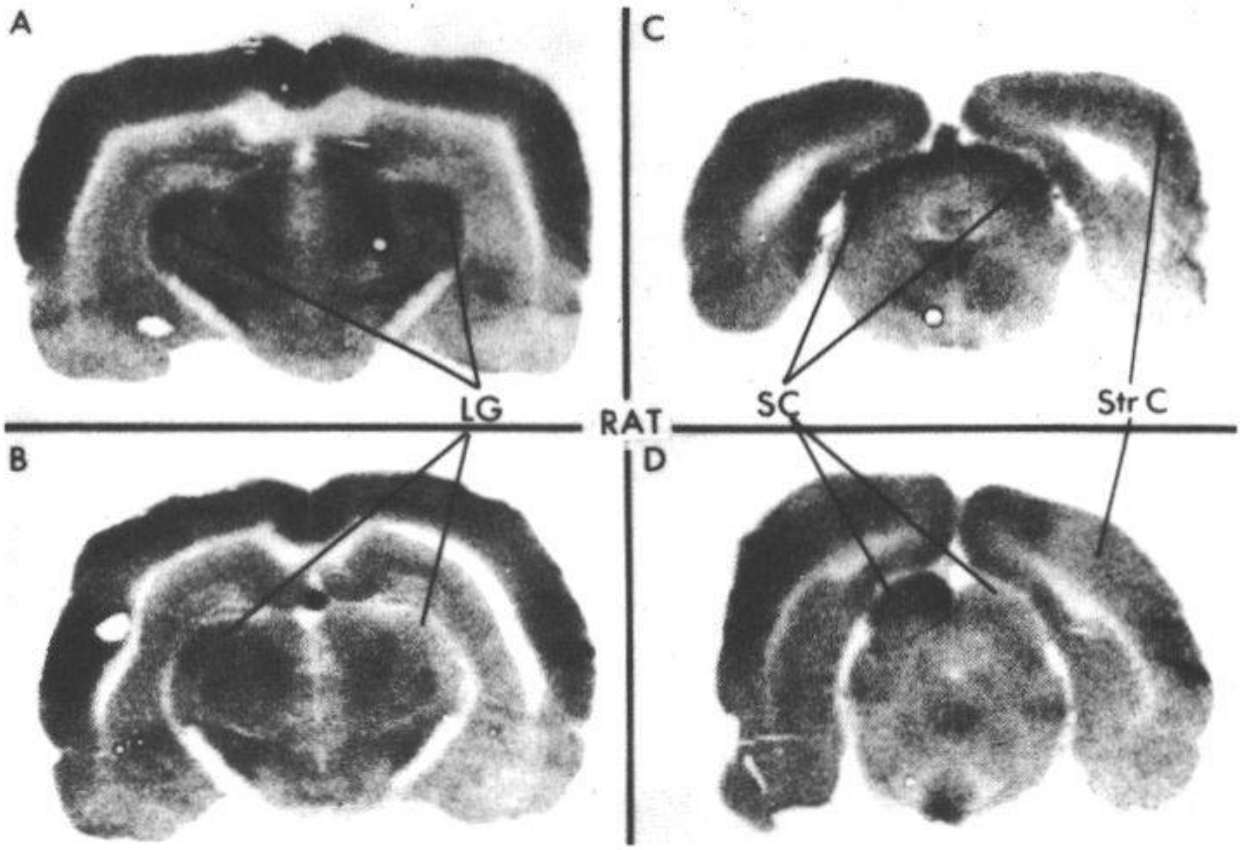

Fig. 3. Effects of unilateral enucleation on (^{14}C)deoxyglucose uptake in components of the visual system in the rat. In the normal rat with both eyes intact the uptakes in the lateral geniculate bodies (LG), superior colliculi (SC) and striate cortex (STR C) are approximately equal on both sides (A and C). In the unilaterally enucleated rat there are marked decreases in optical densities in the areas corresponding to these structures on the side contralateral to the enucleation (B and D). From KENNEDY et al. (1975).

Effects of Decreased Functional Activity

Visual Deprivation in the Rat. Decrements in functional activity result in reduced rates of glucose utilization. In the rat, the visual system is 80-85 % crossed at the optic chiasma (LASHLEY, 1934; MONTERO and GUILLERY, 1968), and unilateral enucleation removes most of the sensory input due to either retinal stimulation by light or spontaneous retinal cell potentials to the central visual structures of the contralateral side. In the conscious rat studied 24 hours after unilateral enucleation, there are marked decrements in (^{14}C)DG uptake in the contralateral superior colliculus, lateral geniculate body, and visual cortex as compared to the ipsilateral side (Fig. 3) (KENNEDY et al. 1975). These effects are observed whether the remaining eye is stimulated repetitively with a photoflash or the animal is maintained in normal room light. In the rat with both eyes intact, no asymmetry in the autoradiographs is observed (Fig. 3).

Visual Deprivation in the Monkey. In animals with binocular visual systems, such as the Thesus monkey, there is only approximately 50 % crossing of the visual pathways, and the structures of the visual system on each side of the brain receive equal inputs from both retinae. Although each retina projects more or less equally to both hemispheres, their projections remain segregated and terminate in six well-defined laminae in the lateral geniculates, three each for the ipsilateral and contralateral eyes (HUBEL and WIESEL, 1968; HUBEL and Wiesel, 1972; WIESEL, HUBEL and LAM, 1974; RAKIC, 1976). This segregation is preserved in the optic radiations which project the monocular representations of the two eyes for any segment of the visual field to adjacent regions of Layer IV of the striate cortex (HUBEL and WIESEL, 1968; HUBEL and WIESEL, 1972). The cells responding to the input of each monocular terminal zone are distributed transversely through the thickness of the striate cortex resulting in a mosaic of columns, 0.3-0.5 mm in width, alternately representing the monocular inputs of the two eyes. The nature and distribution of these ocular dominance columns have previously been characterized by electrophysiological techniques (HUBEL and WIESEL, 1968), Nauta degeneration methods (HUBEL and WIESEL, 1972), and by autoradiographic visualization of axonal and transneuronal transport of (^{3}H)proline- and (^{3}H)fucose-labeled protein and/or glycoprotein (WIESEL, HUBEL and LAM, 1974; RAKIC, 1976).

In order to examine the effects of functional activity on energy metabolism in the binocular visual system, three groups of monkeys with different conditions of visual input were studied: 1) intact binocular vision; 2) bilateral visual occlusion; 3) monocular visual occlusion. Visual occlusions were achieved either by enucleation or by insertion of opaque plastic discs in the appropriate eyes at the time of the surgical procedure for the insertion of the catheters, i.e., 2-4 hours prior to the administration of the pulse of (^{14}C)DG. Animals with intact vision in one or both eyes were either exposed to the ambient light of the laboratory or surrounded by a rotating, illuminated, black-white, complex geometric pattern during the experimental procedure. The results were qualitatively similar with either method of visual occlusion and with or without the rotating geometric pattern. Experimental modification of the visual input produced consistent changes in the pattern of distribution of the rates of glucose consumption, all clearly visible in the autoradiographs, that coincided closely with the changes in functional activity expected from known physiological and anatomic properties of the binocular visual system (KENNEDY et al. 1976).

1) Normal binocular vision. In animals with intact binocular vision no bilateral asymmetry was seen in the autoradiographs of the structures of the visual system (Figs. 4A, 5A). The lateral geniculate bodies and oculomotor nuclei appeared to be of fairly uniform density and essentially the same on both sides (Fig. 4A). The visual cortex was essentially the same on

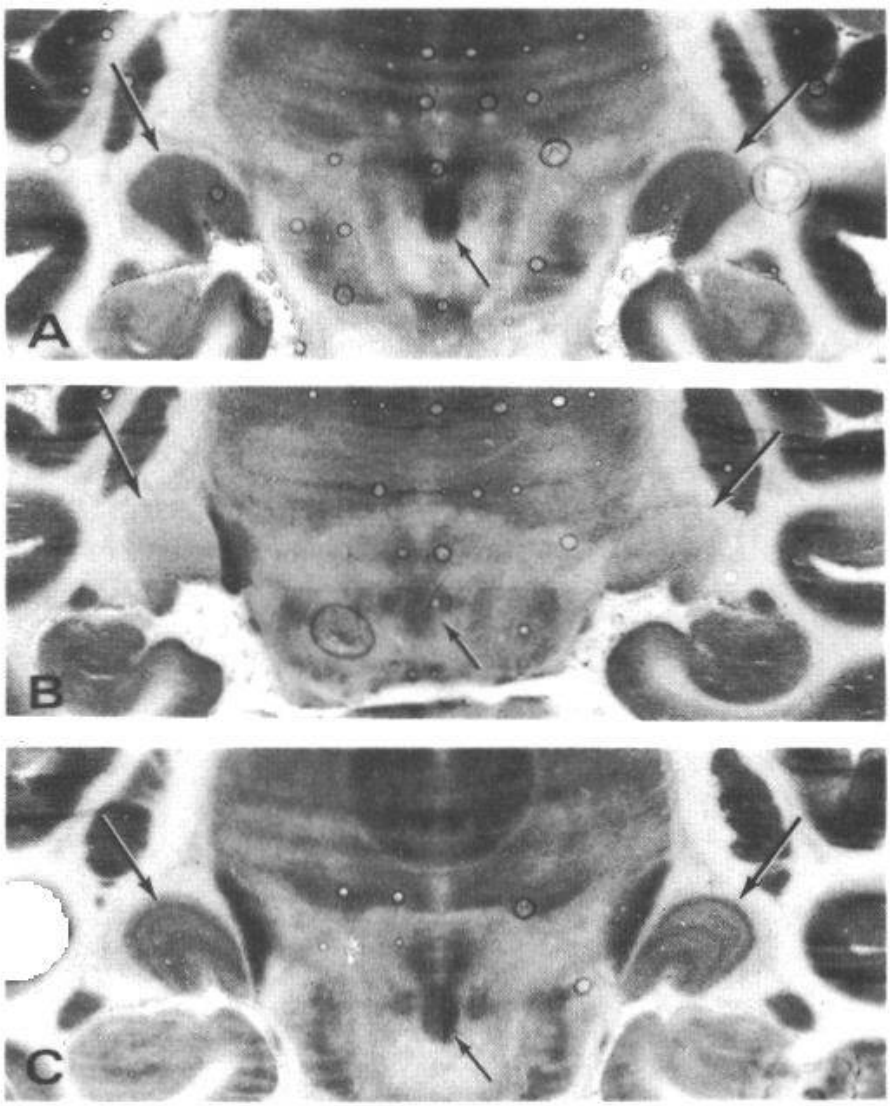

5.0mm

Fig. 4. Autoradiography of coronal brain sections from Rhesus monkeys at the level of the lateral geniculate bodies. Large arrows point to the lateral geniculate bodies; small arrows point to oculomotor nuclear complex. A) Animal with intact binocular vision. Note the bilateral symmetry and relative homogeneity of the lateral geniculate bodies and oculomotor nuclei. B) Animal with bilateral visual occlusion. Note the reduced relative densities, the relative homogeneity, and the bilateral symmetry of the lateral geniculate bodies and oculomotor nuclei. C. Animal with right eye occluded. The left side of the brain is on the left side of the photograph. Note the laminae and the inverse order of the dark and light bands in the two lateral geniculate bodies. Note also the lesser density of the oculomotor nuclear complex on the side contralateral to the occluded eye. From KENNEDY et al. (1976).

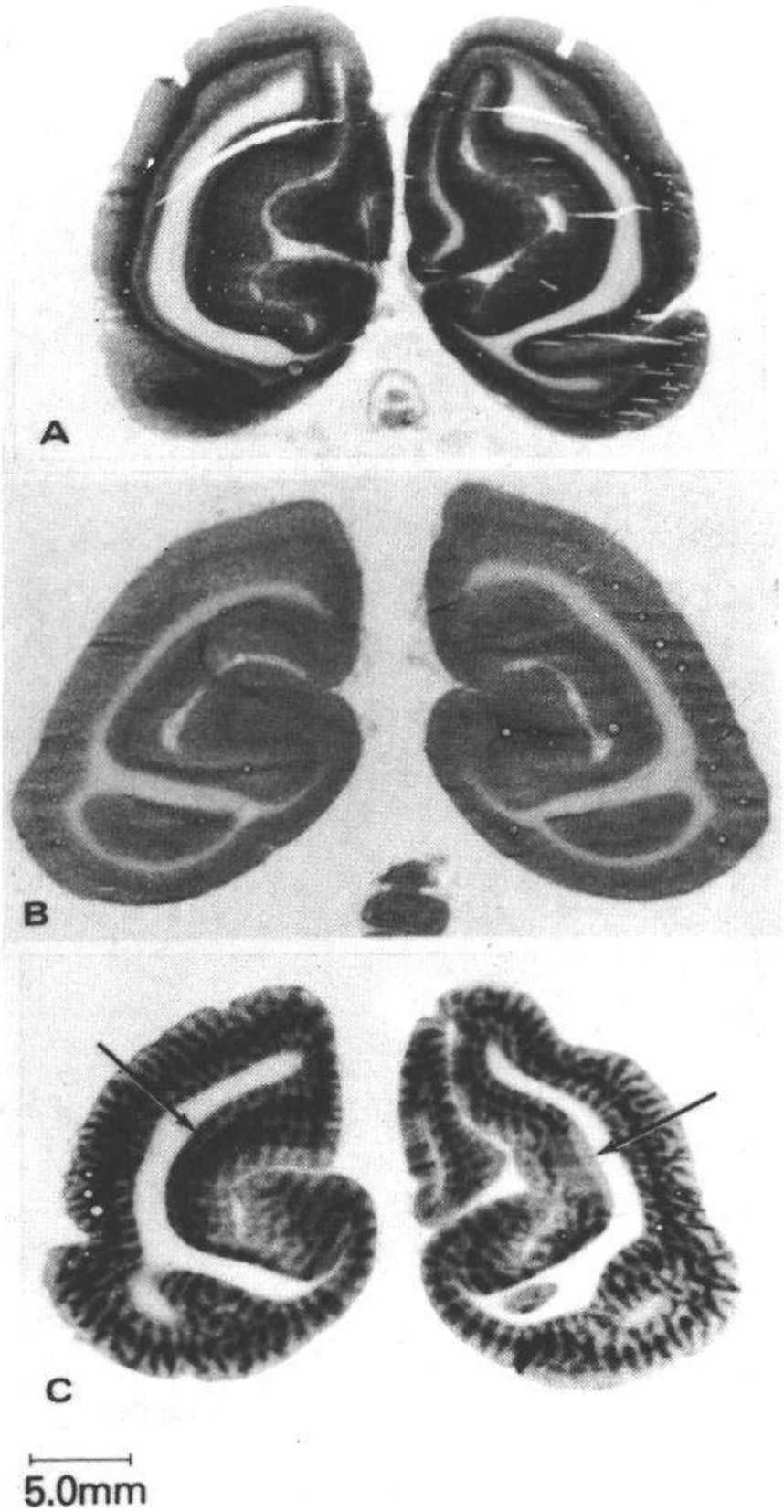

Fig. 5

both sides (Fig. 5A), but throughout all of Area 17 there was heterogeneous density distributed in a characteristic laminar pattern. At least four different levels of density could be readily discerned which could be correlated with the known cytoarchitectural layers of the striate cortex apparent in myelin- and thionin-stained sections (Fig. 6). A wide band of relatively low but uniform density in the autoradiograph encompassed Layers I, II, and III which could not be distinguished further on the basis of (^{14}C)deoxyglucose uptake (Fig. 6). Layers IVa, IVb, and IVc were clearly associated with high rates of glucose utilization as indicated by the density of the autoradiographic regions corresponding to them; Layers IVb and IVc were the most active, exhibiting the densest patterns of all the layers seen in the autoradiograph (Fig. 6). When the autoradiograph is compared with the section stained for myelin, it appears that the line of Gennari lies within the layer with greatest metabolic activity (Fig. 6). In Layer V there appears to be a fairly abrupt decline in density, but the activity in Layer IV is intermediate between those of Layers IV and V (Fig. 6). These observations indicate that in animals with binocular visual input the rates of glucose consumption in the visual pathways are essentially equal on both sides of the brain and relatively uniform in the oculomotor nuclei and lateral geniculate bodies, but markedly different in the various layers of th striate cortex. The most intense metabolic activity appears to be in sub-layers of Layer IV (Figs. 5 A, 6), coinciding with the sites of termination of the geniculocortical projections on spine-bearing stellate cells (HUBEL and WIESEL, 1972; GAREY and POWELL, 1971). Within each layer, or sub-layer, however, the metabolic activity appears to be relatively uniform throughout the extent of the cortex representing the various portions of the visual fields.

Fig. 5. Autoradiographs of coronal brain sections from Rhesus monkeys at the level of the striate cortex. A) Animal with normal binocular vision. Note the laminar distribution of the density; the dark band corresponds to Layer IV. B) Animal with bilateral visual deprivation. Note the almost uniform and reduced relative density, especially the virtual disappearance of the dark band corresponding to Layer IV. C) Animal with right eye occluded. The half-brain on the left side of the photograph represents the left hemisphere contralateral to the occluded eye. Note the alternate dark and light striations, each approximately 0.3-0.4 mm in width, representing the ocular dominance columns. These columns are most apparent in the dark lamina corresponding to Layer IV but extend through the entire thickness of the cortex. The arrows point to regions of bilateral asymmetry where the ocular dominance columns are absent. These are presumably areas with normally only monocular input. The one on left, contralateral to occluded eye, has a continuous dark lamina corresponding to Layer IV which is completely absent on the side ipsilateral to the occluded eye. These regions are believed to be the loci of the cortical representations of the blind spots (see text). From KENNEDY et al. (1976).

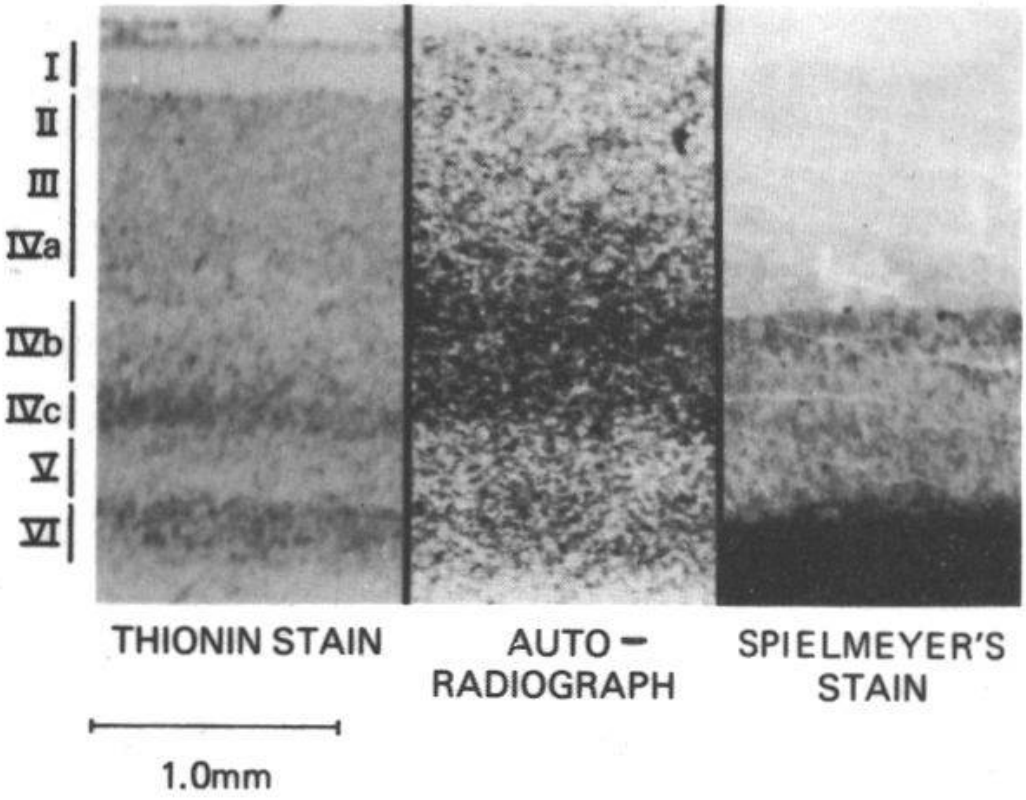

Fig. 6. Comparison of autoradiograph, thionin stain, and myelin stain of a section of striate cortex from a monkey with intact binocular vision. The autoradiograph was made from the same section subsequently stained with thionin. An immediately adjacent section was stained for myelin with Spielmeyer's stain. The thionin stain distinguishes the cell-sparse Layers I, IVb, and V and the three cell-dense regions, Layers II, III and IVa (considered as one), Layer IVc, and Layer VI, according to Brodman's system. The dense zone in the autoradiograph traverses all of Layer IV and encompasses the stria of Gennari which is demarcated by the myelin stain. From KENNEDY et al. (1976).

2. Bilateral visual deprivation. Autoradiographs from the animals with both eyes occluded exhibited generally decreased labeling of all components of the visual system, but the bilateral symmetry was generally retained (Figs. 4B, 5B), and the density within each lateral geniculate body was for the most part fairly uniform (Fig. 4B). In the striate cortex, however, the marked differences in the densities of the various Layers seen in the animals with intact bilateral vision (Fig. 5A) were virtually absent so that, except for a faint delineation of a band within Layer IV, the concentration of the label was essentially homogeneous throughout the striate cortex (Fig. 5B).

3) Unilateral visual deprivation. Autoradiographs from monkeys with only monocular input exhibited markedly different patterns from those described above. Both lateral geniculate bodies exhibited exactly inverse patterns of alternating dark and light bands corresponding to the known laminae representing the regions receiving the different inputs from the

retinae of the intact and occluded eyes (Fig. 4C). Bilateral asymmetry was also seen in the oculomotor nuclear complex; a lower density was apparent in the nuclei contralateral to the occluded eye (Fig. 4C). In the striate cortex the pattern of distribution of the (^{14}C) deoxyglucose-6-phosphate appeared to be a composite of the patterns seen in the animals with intact and bilaterally occluded visual input. The pattern found in the former regularly alternates with that of the latter in columns oriented perpendicularly to the cortical surface (Fig. 5C). The dimensions, arrangement, and distribution of these columns are identical to those of the ocular dominance columns described by HUBEL and WIESEL (1968; 1972) and WIESEL, HUBEL and LAM (1974). These columns reflect the interdigitation of the representations of the two retinae in the visual cortex. Each element in the visual field is represented by a pair of contiguous bands in the visual cortex, one for each of the two retinae or their portions that correspond to the given point in the visual fields. With symmetrical visual input bilaterally, the columns representing the two eyes are equally active and, therefore, not visualized in the autoradiographs (Fig. 5A). When one eye is blocked, however, only those columns representing the blocked eye become metabolically less active, and the autoradiographs then display the alternate bands of normal and depressed activities corresponding to the regions of visual cortical representation of the two eyes (Fig. 5C).

There can be seen in the autoradiographs from the animals with unilateral visual occlusion regions in the folded calcarine cortex that exhibit bilateral asymmetry (Fig. 5C). The ocular dominance columns are absent on both sides, but on the side contralateral to the occluded eye this region has the appearance of visual cortex from an animal with normal bilateral vision, and on the ipsilateral side this region looks like cortex from an animal with both eyes occluded (Fig. 5). These regions are the loci of the cortical representation of the blind spots of the visual fields and normally have only monocular input (KENNEDY et al. 1975). The area of the optic disc in the nasal half of each retina cannot transmit to this region of the contralateral striate cortex which, therefore, receives its sole input from an area in the temporal half of the ipsilateral retina. Occlusion of one eye deprives this region of the ipsilateral striate cortex of all input while the corresponding region of the contralateral striate cortex retains uninterrupted input from the intact eye. The metabolic reflection of this ipsilateral monocular input is seen in the autoradiographs in Fig. 5C.

Relationship between local energy metabolism and local blood flow in the brain

The availability of methods for measuring both glucose utilization and blood flow in individual discrete structural components of the brain has made it possible to examine directly the relationship between them. The results demonstrate that they are indeed closely related

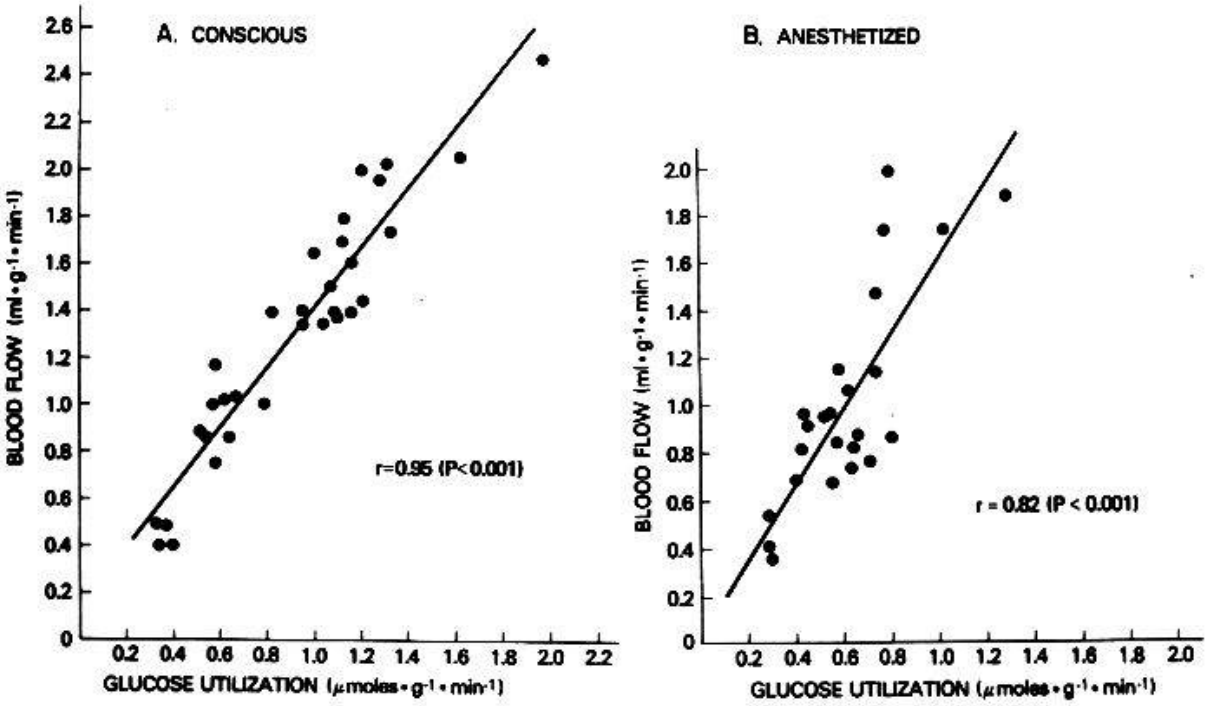

Fig. 7. Correlation between local cerebral blood flow, measured with the (^{14}C)iodoantipyrine technique (SAKURADA et al. 1978), and local cerebral glucose utilization, measured with the (^{14}C)deoxyglucose technique (SOKOLOFF et al. 1977). Each point represents a different structure in the brain. A) Normal conscious rat. Each point represents the mean local glucose utilization obtained from 10 rats and the mean local blood flow obtained from 6 rats. B) Thiopental anesthesia. Each point represents the mean values of local glucose utilization and blood flow obtained from 8 animals and 6 animals, respectively. From M.H. DES ROSIERS, O. SAKURADA, M. SHINOHARA, C. KENNEDY, and L. SOKOLOFF, (unpublished observations).

(DES ROSIERS et al. 1974). In the normal conscious rat the coefficient of correlation between the rates of glucose utilization and blood flow in the various cerebral structures is equal to 0.95 ($p < 0.001$) (Fig. 7A). Thiopental anesthesia reduces the rates of both metabolism and blood flow in almost all the structures, but the correlation, though reduced, still remains quite close ($r = 0.80$, $p < 0.001$) (Fig. 7B). These results confirm that the individual cerebral structures are normally perfused more or less in proportion to their metabolic demands.

Not only do the rates of blood flow in the various structural components of the brain normally parallel the local rates of glucose consumption, but local blood flow is generally altered, just as local energy metabolism is, in response to changes in local functional activity. Local blood flow is measured with an autoradiographic technique like that of the (^{14}C)deoxyglucose technique that demonstrates the relative rates of blood flow in the various cerebral structures. These autoradiographs demonstrate that the same structures that exhibit changes in glucose

utilization also exhibit comparable changes in blood flow in altered physiological states. For example, retinal stimulation with a photoflash produces increased blood flow in discrete regions of the visual cortex, lateral geniculate body and superior colliculus of the conscious cat (SOKOLOFF 1961). Unilateral enucleation in the rat reduces blood flow and glucose utilization contralaterally in these structures (Fig. 3); indeed the autoradiographs obtained with (^{14}C)iodoantipyrine are then almost indistinguishable from those obtained with (^{14}C)-deoxyglucose (M. H. DES ROSIERS, unpublished observations). Focal seizures produced by the application of penicillin to the motor cortex in the monkey result in local increases in blood flow in the same structures that exhibit increased glucose consumption (Fig. 2) (CAVENESS et al. 1975).

It is clear from the results of the studies of local cerebral blood flow and glucose utilization that energy metabolism and functional activity are closely coupled in the nervous system and that local blood flow is distributed and adjusted in the cerebral tissues to local metabolic demand and thereby to local functional activity. The results fully confirm the hypothesis of ROY and SHERRINGTON (1890), but the mechanisms responsible for the close coupling of these functions remain unknow.

Summary

The results of studies with the (^{14}C)deoxyglucose technique unequivocally establish that local energy metabolism in cerebral tissues is, as in other tissues, closely coupled to local functional activity. Stimulation of local functional activity increases the local rate of glucose utilization; reduced functional activity depresses it. Local cerebral blood flow is normally distributed among the cerebral structures in almoust exact proportion to their rates of glucose utilization and changes together with local glucose consumption in response to altered local functional activity. These results demonstrate that the level of functional activity in the structural and functional components of the central nervous system regulates the local rate of energy metabolism, and local blood flow is adjusted to the local metabolic demand.

Caveness W.F. (1969): Ontogeny of focal seizures. In: Basic Mechanisms of the Epilepsies. Edited by H.H. Jasper, A.A. Ward and A Pope. Boston. Little, Brown and Co., pp. 517-534.

Caveness W.F., Ueno H. and Kemper T.L. (1975): Subcortical factors in experimental Jacksonian seizures. In: 7th International Congress Neuropathol. Proc., Vol. 2. Edited by S. Kornyey, S. Tariska, and G. Gosztonyi. Amsterdam: Excerpta Medica, pp. 29-34.

Collins R.C., Kennedy C., Sokoloff L. and Plum F. (1976): Metabolic anatomy of focal motor seizures. Arch. Neurol. 33, 536-542.

Des Rosiers M.H., Kennedy C., Patlak C.S., Pettigrew K.D., Sokoloff L., and Reivich M. (1974): Relationship between local cerebral blood flow and glucose utilization in the rat. Neurol. 24 (4), 389.

Eckman W.W., Phair R.D., Fenstermacher J.D., Patlak C.S., Kennedy C., and Sokoloff L. (1975): Permeability limitation in estimation of local brain blood flow with (^{14}C)antipyrine. Am. J. Physiol. 229, 215-221.

Eklöf B., Lassen N.A., Nilsson L., Norberg K., and Siesjö B.K. (1973): Blood flow and metabolic rate for oxygen in the cerebral cortex of the rat. Acta Physiol. Scand. 88, 587-589.

Freygang W.H. Jr. and Sokoloff L. (1958): Quantitative measurement of regional circulation in the central nervous system by the use of radioactive inert gas. Adv. in Biol. and Med. Physics 6, 263-279.

Garey L.J. and Powell T.P.S. (1971): An experimental study of the termination of the lateral geniculo-cortical pathway in the cat and monkey. Proc. Royal Soc. London 179, 41-63.

Hubel D.H. and Wiesel T.N. (1968): Receptive fields and functional architecture of monkey striate cortex. J. Physiol. 195, 215-243.

Hubel D.H. and Wiesel T.N. (1972): Laminar and columnar distribution of geniculo-cortical fibers in the Macaque monkey. J. Comp. Neurol. 146, 421-450.

Kennedy C., Des Rosiers M., Jehle J.W., Reivich M., Sharp F. and Sokoloff L. (1975): Mapping of functional neural pathways by autoradiographic survey of local metabolic rate with (^{14}C)deoxyglucose. Science 187, 805-853.

Kennedy C., Des Rosiers M.H., Sakurada O., Shinohara M., Reivich M., Jehle J.W., and Sokoloff L. (1976): Metabolic mapping of the primary visual system of the monkey by means of the autoradiographic (^{14}C)deoxyglucose technique. Proc. Natl. Acad. Sci. USA 73, 4230-4234.

Kennedy C., Sakurada O., Shinohara M., Jehle J., and Sokoloff L. (1978): Local cerebral glucose utilization in the normal conscious Macaque monkey. Ann. Neurol. 4, 293-301.

Landau W.M., Freygang W.H. jr., Rowland L.P., Sokoloff L. and Kety S.S. (1955) The local circulation of the living brain; values in the unanestetized and anesthetized cat. Trans. Amer. Neurol. Assoc. 80, 125-129.

Lashley K.S. (1934): The mechanism of vision. VII. The projection of the retina upon the primary optic centers of the rat. J. Comp. Neurol. 59, 341-373.

Montero V.M. and Guillery R.W. (1968): Degeneration in the dorsal lateral geniculate nucleus of the rat following interruption of the retinal or cortical connections. J. Comp. Neurol. 134, 211-242.

Nilsson B. and Siesjö B.K. (1976): A method for determining blood flow and oxygen consumption in the rat brain. Acta Physiol. Scand. 96, 72-82.

Rakic P. (1976): Prenatal genesis of connections subserving ocular dominance in the Rhesus monkey. Nature 261, 467-471.

Reivich M., Jehle J., Sokoloff L., and Kety S.S. (1969): Measurement of regional cerebral blood flow with antipyrine-^{14}C in awake cats. J. Appl. Physiol. 27, 296-300.

Roy C.W. and Sherrington C.S. (1890): On the regulation of the bloodsupply of the brain. J. Physiol., 11, 85-108.

Sakurada O., Kennedy C., Jehle J., Brown J.D., Carbin G.L., and Sokoloff L. (1978): Measurement of local cerebral blood flow with (^{14}C)iodoantipyrine. Amer. J. Physiol. 234(1), H59-H66.

Schmidt C.F., Kety S.S. and Pennes H.H. (1945): The gaseous metabolism of the brain of the monkey. Amer. J. Physiol. 143, 33-52.

Sokoloff L. (1961): Local cerebral circulation at rest and during altered cerebral activity induced by anesthesia or visual stimulation. In: The Regional Chemistry, Physiology and Pharmacology of the Nervous System. Edited by S.S. Kety and J. Elkes. Oxford: Pergamon Press, Ltd., pp. 107-117.

Sokoloff L. (1977): Relation between physiological function and energy metabolism in the central nervous system. J. Neurochem. 29, 13-26.

Sokoloff L. (1979): The (^{14}C)deoxyglucose method: four years later. In: Cerebral Blood Flow and Metabolism. Edited by F. Gotoh, H. Nagai, and Y. Tazaki. Copenhagen: Munksgard, pp. 640-649.

Sokoloff L., Reivich M., Kennedy C., Des Rosiers M.H., Patlak C.S., Pettigrew K.D., Sakurada O., and Shinohara M. (1977): The (^{14}C)deoxyglucose method for the measurement of local cerebral glucose utilization: theory, procedure, and normal values in the conscious and anesthetized albino rat. J. Neurochem. 28, 897-916.

Wiesel T.N., Hubel D.H., and Lam D.M.K. (1974): Autoradiographic demonstration of ocular dominance columns in the monkey striate cortex by means of transneuronal transport. Brain Res. 79, 273-279.

Correspondence to: Dr. Louis Sokoloff, NIMH, Bldg. 36, Rm. 1A-27, 9000 Rockville Pike, Bethesda, Maryland 20205 (U.S.A.)